Pilot Symbol Transmission for Time-Varying Fading Channels: An Information-Theoretic Optimization

Parastoo Sadeghi, Yang Liu, and Rodney A. Kennedy
ANU College of Engineering and Computer Science
The Australian National University
Canberra 0200 ACT, Australia
{parastoo.sadeghi};{yang.liu};{rodney.kennedy}@anu.edu.au

Predrag B. Rapajic
School of Engineering
University of Greenwich at Medway
KENT ME4 4TB United Kingdom
p.rapajic@greenwich.ac.uk

***Abstract*— We consider the optimal design of pilot-symbol-assisted modulation (PSAM) in time-varying flat-fading channels (FFC). The FFC is modeled as an autoregressive Gauss-Markov random process, whose realization is unknown at the transmitter or at the receiver. Our measure of optimality for channel estimation is the rate of information transfer through the channel. The parameters that are available for this optimization are the power ratio and the fraction of time that are allocated to pilot transmission. Our approach is different from (and builds upon) a recent study of PSAM for the Gauss-Markov FFC, where the aim was to minimize the maximum steady-state minimum mean square error (MMSE) of channel estimation for equal power allocated to pilot and data symbols and for a fixed pilot insertion ratio. To this end, we examine a lower bound on the capacity and find the optimal pilot transmission parameters that maximize this bound. Our analysis shows that this capacity lower bound is more sensitive to the pilot power allocation ratio in relatively slow fading channels (with the normalized fading rate $f_D T_s \simeq 0.01$). We observe that for such slow fading rates, optimal power allocation and optimal pilot spacing are more sensitive to the operating SNR. Another finding is that equal power allocation strategy is suboptimal by at most 1 dB for the slow fading rate of $f_D T_s \simeq 0.01$.**

Keywords — Pilot-symbol-assisted modulation, Time-varying flat-fading channels, Channel estimation, Channel information capacity, Capacity lower bounds.

I. Introduction

A. Motivation and Background

Pilot-symbol-assisted modulation (PSAM) [1] refers to periodic transmission of known symbols to the receiver to assist estimation of unknown channel parameters, such as the phase or magnitude of the channel gain. Since its introduction in late 1980s and early 1990s, PSAM has been widely used in practical wireless communications over multipath fading channels, such as in the Global System for Mobile Communications (GSM) [2]. Although channel estimation and hence, reliable data decoding is facilitated through pilot symbol transmission, this often comes at a considerable cost in the form of reduction in the information capacity. For the GSM example, 26 known bits in every 156 bits are allocated to pilot transmission. Since pilot bits do not carry information, this immediately results in about 17% reduction in the capacity. Further reduction in the capacity is due to errors in channel estimation. Such early designs were simple and somewhat ad-hoc examples of PSAM, which did not aim to maximize the achievable information rate through the wireless channel.

The effect of imperfect knowledge of the wireless channel (using probe or pilot signals) on the information capacity was first studied in [3]. It was shown in [3] that the imperfect channel knowledge will manifest itself in the form of reduced signal-to-noise ratio (SNR) in a capacity lower bound. However, it was assumed in [3] that the "probe" signal for channel estimation occupies its own band and does not overlap in the frequency of the information carrying signal. Whereas in the PSAM scheme, pilot symbols occupy the same frequency band as data symbols and take up valuable transmission time and power. Therefore, one could not immediately employ the results for determining achievable information rates in practical PSAM systems.

Following [3], the aim of more recent studies including [4]–[7] has been to maximize either the achievable information rate or the capacity lower bound in PSAM transmission. Three main optimizable system parameters in PSAM are as follows

- the ratio of the transmitter power allocated to pilot symbols, denoted by γ
- the fraction of time allocated to pilot symbols (also known as pilot spacing or frequency), denoted by η
- the arrangement of pilot symbols, *i.e.* whether they should be clustered together or spread among data symbols

Based on the contributions in [4]–[7], it is now known that the clustering of pilot symbols is not a wise thing to do, which may result in inferior capacity performance. It is also known that allocation of equal power to individual pilots and data symbols can be suboptimal, which may result in capacity reduction. The fact that pilot symbols should be spread among data symbols was also confirmed in the work of [8], where the optimality criterion was minimizing the maximum steady-state minimum mean square error (MMSE) of channel estimation in Gauss-Markov FFCs.

The fading channel model or the communication setup plays an important role on how PSAM performs and on its optimal design. For example, [4], [5] considered the effect of pilot power allocation and spacing on a capacity lower bound in band-limited fading processes with a low-pass Doppler power spectrum (such as Clarke's fading model [9]). Since the fading

process was assumed to be band-limited, the authors concluded that minimal sampling of the fading process with the Nyquist rate is optimal. On the other hand, the study of information rates with perfect interleaving in [7] concludes that pilot symbols should be sent more frequently than the Nyquist rate, especially for slower fading channels. The authors in [6] considered optimal PSAM design in block fading channels and multiple-antenna communications. Under the block fading assumption, the fading channel process is fixed, but unknown to the receiver for a period of N symbols and then changes to an independent value in the next block. It was concluded that in the single antenna setup and when the pilot power is optimized, only one training symbol per block should be sent to maximize the capacity lower bound.

The band-limited fading and the block fading assumptions considered in [4]–[7] both imply a strong correlation in the channel amplitude and phase over a block of transmitted symbols. The Gauss-Markov fading model is an alternative model for time-varying fading channels, which is widely used for characterizing the fading process [3], [10]. Roughly speaking, the fading process in a Gauss-Markov channel is more random, less predictable and less correlated than a band-limited fading channel (with an infinite memory order [11]).

B. Approach and Contributions

In this paper, we optimize the capacity lower bound for PSAM transmission in time-varying Gauss-Markov fading channels. Our contributions build upon a recent study in [8], where the authors minimized the maximum steady-state MMSE for channel estimation in Gauss-Markov fading channels for a *fixed* pilot spacing or frequency and for *equal* power allocated to individual pilot and data symbols. However, our approach is different from [8] in the sense that we allow the pilot power ratio and spacing to vary and optimize these parameters to maximize a lower bound on the capacity. Our work is also an extension of [3] in the sense that we investigate information rates that are practically achievable using "in-band" pilot transmission for the Gauss-Markov fading channels.

Three contributions of this paper are summarized as follows.

1) In Section V, we derive the lower bound on the channel capacity for Gauss-Markov fading channels in PSAM scheme. This lower bound is based on the steady-state MMSE of channel estimation and prediction in the pilot and data transmission modes, respectively, using the Kalman filter. The parameters in this derivation are the pilot power ratio γ and pilot spacing η.
2) In Section VI, we investigate optimal allocation of power to pilot symbols to maximize the derived capacity lower bound. We find that the capacity lower bound is more sensitive to the allocation ratio of power to pilot symbols in slow fading channels (for example at the normalized fading rate of $f_D T_s \simeq 0.01$) than in faster fading channels. We observe that for such slow fading rates, optimal power allocation is more sensitive to the operating SNR. We compare the capacity lower bound at the optimal pilot power allocation with that using equal power allocation scheme. We observe that equal power allocation scheme incurs about 1 dB capacity loss for the slow fading channel ($f_D T_s \simeq 0.01$). However, for faster fading channels the capacity loss is negligible, which warrants the use of simple equal power allocation scheme. We also examine whether an alternative *power ramping* strategy (see Section III-D for the definition) results in any improvement in the capacity lower bound.
3) In Section VI, we investigate optimal pilot spacing or frequency to maximize the derived capacity lower bound. Our first observation in this analysis is that the optimal pilot spacing is sensitive to the operating SNR in slow fading channels with $f_D T_s \simeq 0.01$. Second, for fast fading channels (the normalized fading rate of $f_D T_s \gtrsim 0.1$), very frequent pilots or equivalently, very short block lengths are required to maximize the capacity lower bound.

II. Fading Channel Model

The wireless channel is a correlated, time-varying, and flat-fading channel (FFC), which is defined as

$$y_\ell = g_\ell x_\ell + n_\ell, \tag{1}$$

where n_ℓ is the complex-valued additive white Gaussian noise (AWGN) with variance per dimension $N_0/2$ and independent real and imaginary components. $g_\ell = a_\ell e^{j\theta_\ell}$ is the Gaussian-distributed FFC gain, with Rayleigh-distributed FFC amplitude a_ℓ and uniformly-distributed FFC phase θ_ℓ. The variance of complex g_ℓ is denoted by σ_g^2. We assume that the average data and pilot symbol powers are $\mathcal{E}_d$ and $\mathcal{E}_p$, respectively. Therefore, the average SNR per symbol in data and pilot transmission modes is $\rho_d = \sigma_g^2 \mathcal{E}_d / N_0$ and $\rho_p = \sigma_g^2 \mathcal{E}_p / N_0$, respectively.

The actual realization of the time-varying FFC gain g_ℓ is unknown to the receiver and to the transmitter *a priori*. It is assumed, however, that the statistics of the time-varying FFC gain g_ℓ are known and do not change over time. Hence, the fading process is stationary. We use the Gauss-Markov process to model time variations of the FFC. The Gauss-Markov process is widely accepted for such modeling [3], [10] and the evolution of the FFC is given as follows

$$g_\ell = \alpha g_{\ell-1} + w_\ell, \tag{2}$$

where w_ℓ is the complex-valued and white Gaussian process noise. The real coefficient $0 \leq \alpha < 1$ in (2) determines the correlation of the fading channel gain at two successive time indices. A small α models a fast fading channel and a large α models a slow fading channel. We assume that this correlation coefficient is determined from the Doppler spread of the channel and is given as $\alpha \triangleq E\{G_\ell G_{\ell-1}^*\}/\sigma_g^2 = J_0(2\pi f_D T_s)$, which is the first normalized correlation coefficient in the band-limited Clarke's model [9], [12]. J_0 is the zero-order Bessel function of the first kind, f_D is the Doppler frequency shift, T_s is the transmitted symbol period, and the superscript $*$ denotes complex conjugate. Moreover, according to the

Clarke's model, we note that the real and imaginary parts of the fading process g_ℓ and those of the process noise w_ℓ are independent of each other. Since we assumed that the statistics of the time-varying FFC gain do not change over time, we can assume that α is known. This is the case, for example, where the mobile unit is moving at a constant (or close to constant) velocity.

III. Pilot Transmission Scheme

A. Pilot Insertion Arrangement

The authors in [8] studied optimal insertion of pilot symbols in Gauss-Markov FFCs. After the transmission of pilot symbol(s), the MMSE of channel prediction using the Kalman method increases as we proceed through the data symbol transmission. Therefore, the largest steady-state MMSE is the one at the end of the data transmission mode. It was shown in [8] that for a fixed ratio of pilot insertion such as η[1], the optimal arrangement of periodic pilot symbols that minimizes this maximum steady-state MMSE of channel estimation is the one with only one periodic pilot symbol followed by a block of data symbols. In other words, pilot symbols should not be clustered together. Instead, they should be spread as evenly among data symbols as possible (while maintaining the required ratio of pilot insertion). Although this conclusion was made under the assumption that pilot and data symbols are allocated equal power, this is in accordance with similar findings in [4]–[7] for band-limited or block FFCs under varying power allocations schemes.

Later in Section V, we will observe that a lower MMSE for channel estimation results in a higher effective SNR per symbol for data decoding. A higher effective SNR per symbol will, in turn, increases a lower bound on the channel capacity. Therefore, it is wise to use the pilot insertion scheme that minimizes the MMSE of channel estimation. Throughout the analysis, we will use the single pilot symbol insertion scheme for the transmission block.

B. Pilot Spacing or Frequency

According to the above discussion, we assume that one pilot symbol is followed by $T-1$ data symbols, making the total transmission block length equal to T symbols. Therefore, the pilot spacing is

$$\eta = \frac{1}{T}, \tag{3}$$

and the ratio of data symbol is

$$1-\eta = \frac{T-1}{T}. \tag{4}$$

C. Pilot Power Allocation

Let us assume that the transmitter has a total available power budget of $\mathcal{E}\times T$ for the transmission of T symbols. As defined in Section II, the average power per data and pilot symbols is $\mathcal{E}_d$ and $\mathcal{E}_p$, respectively. From the conservation of time and energy, we have that

$$\mathcal{E}\times T = \mathcal{E}_p \times 1 + \mathcal{E}_d \times (T-1). \tag{5}$$

Now assume that a fraction of γ of the power budget is allocated for the transmission of one pilot symbol. That is,

$$\mathcal{E}_p = \gamma \mathcal{E} \times T, \tag{6}$$

where $0 \le \gamma \le 1$ and the remaining fraction $(1-\gamma)$ is used for the transmission of $T-1$ data symbols. That is,

$$\mathcal{E}_d \times (T-1) = (1-\gamma)\mathcal{E}\times T. \tag{7}$$

By referring to (3), we conclude that

$$\mathcal{E}_p = \frac{\gamma}{\eta}\mathcal{E}, \tag{8}$$

$$\mathcal{E}_d = \frac{1-\gamma}{1-\eta}\mathcal{E}. \tag{9}$$

Therefore, the average received pilot and data symbol SNRs will be given as

$$\rho_p = \frac{\gamma}{\eta}\frac{\sigma_g^2\mathcal{E}}{N_0} = \frac{\gamma}{\eta}\rho, \tag{10}$$

$$\rho_d = \frac{1-\gamma}{1-\eta}\frac{\sigma_g^2\mathcal{E}}{N_0} = \frac{1-\gamma}{1-\eta}\rho, \tag{11}$$

where $\rho = \sigma_g^2\mathcal{E}/N_0$ and is referred to as the SNR budget.

D. Two Alternative Power Allocation Strategies

We will also consider two alternative pilot power allocation strategies. The first strategy is the equal power strategy between data and pilot modes and is very easy to implement. However, this strategy might be suboptimal in terms of achieving higher information rates through the channel. Therefore, it is of practical significance to know the penalty that we pay in using such a suboptimum strategy, when compared to the optimal power allocation to pilot symbols. In the equal power strategy, we have $\mathcal{E}_p = \mathcal{E}_d$, which according to (8)-(9) results in $\gamma = \eta$. Therefore, for maximizing the capacity lower bound, we only need to optimize over the pilot spacing η.

The second pilot power allocation scheme is a new one, in which the power of data symbols is allowed to 'ramp up' or 'ramp down' during the data transmission block. As will be seen in Section V, in PSAM transmission scheme, the effective SNR is both linearly and inversely affected by the signal power (see (25)). The effective SNR, in turn, affects the capacity of PSAM scheme. If we keep the data power constant during the data block transmission, the effective SNR decreases as we proceed. Here, we are interested to know if we can counter this reduction in the effective SNR by allowing a linearly varying data symbol power in the block. In particular, let us assume that the data symbol power $\mathcal{E}_d$ is a function of time index ℓ. To reflect this, we rewrite (5) as

$$\mathcal{E}T = \mathcal{E}_p \times 1 + \sum_{\ell=2}^{T}\mathcal{E}_d(\ell). \tag{12}$$

[1]The ratio η is also known as pilot spacing or frequency, which are interchangeably used in the paper.

Let us further assume that the data symbol power $\mathcal{E}_d(\ell)$ follows a geometric series as

$$\mathcal{E}_d(\ell) = \beta^{(\ell-2)}\mathcal{E}_d(2), \quad 2 \le \ell \le T, \tag{13}$$

where β can be any positive-valued power ramping parameter. By using $\mathcal{E}_p = \gamma E \times T$, (3), and (13) in (12), we obtain

$$\mathcal{E}_d(2) = \frac{1-\beta}{1-\beta^{(\frac{1}{\eta}-1)}}\frac{(1-\gamma)}{\eta}\mathcal{E}. \tag{14}$$

Later in Section VI, we will evaluate the performance of this ramping power allocation scheme.

IV. Channel Estimation Scheme

The Gauss-Markov model for the FFC given in (2) lends itself very well for recursive and linear MMSE channel estimation at the receiver using the Kalman filter. In this section, we review the main results in [8], which are required later in Section V.

Let the channel estimate obtained from the Kalman filter be denoted by $\hat{g}$ and the channel estimation error be denoted by $\tilde{g}$. The Kalman filter is a linear MMSE estimator, which yields

$$g = \hat{g} + \tilde{g}, \tag{15}$$

where the steady-state MMSE of channel estimation in the pilot transmission mode (time index $\ell = 1$) is derived from the Riccati equation to be

$$M(1) \triangleq \sigma^2_{\tilde{g}}(1) \tag{16}$$

$$= \frac{\sigma_g^2}{\frac{1}{2}(1+\rho_p) + \sqrt{\left[\frac{1}{2}(1+\rho_p)\right]^2 + \frac{\alpha^{\frac{2}{\eta}}}{1-\alpha^{\frac{2}{\eta}}}\rho_p}}, \tag{17}$$

where ρ_p was defined in (10).

After transmission of the single pilot symbol and in data transmission mode (time index $2 \le \ell \le T$), the Kalman filter can only predict (and not filter) the channel. Therefore, it produces increasingly unreliable estimates of the FFC gain $\hat{g}$. The MMSE of channel estimation at the end of each block (the last data symbol) is the largest and given as

$$M(T) \triangleq \sigma^2_{\tilde{g}}(T) = \sigma_g^2 - \alpha^{\frac{2(1-\eta)}{\eta}}(\sigma_g^2 - M(1)). \tag{18}$$

For other data symbols between $2 \le \ell < T$, the channel estimation MMSE is given as

$$M(\ell) \triangleq \sigma^2_{\tilde{g}}(\ell) = \frac{M(T) - \sigma_g^2\big(1-\alpha^{2(\frac{1}{\eta}-\ell)}\big)}{\alpha^{2(\frac{1}{\eta}-\ell)}}, \tag{19}$$

where upon replacing $M(T)$ from (18) in (19) and simplifying we obtain

$$M(\ell) = \sigma_g^2 - \alpha^{2(\ell-1)}\big(\sigma_g^2 - M(1)\big). \tag{20}$$

Since $M(1) \le \sigma_g^2$ and $\alpha < 1$, we conclude that $M(\ell)$ is an increasing function of ℓ. Based on the variance of channel estimation error $M(\ell)$, the variance of channel estimate $\sigma^2_{\hat{g}}$ at any time index ℓ in the block is given as

$$\sigma^2_{\hat{g}}(\ell) = \sigma_g^2 - M(\ell)$$
$$= \alpha^{2(\ell-1)}\big(\sigma_g^2 - M(1)\big), \tag{21}$$

which results from the fact that the channel estimation error is orthogonal to the estimated value.

Before we conclude this section, we note that in Kalman prediction, the channel estimate at time index ℓ during data transmission is related to the channel estimate at time index $\ell - 1$ through [8]

$$\hat{g}_\ell = \alpha \hat{g}_{\ell-1}.$$

Therefore, we obtain the following relation between the channel estimate $\hat{g}_\ell$ and the first channel estimate $\hat{g}_1$ at pilot transmission

$$\hat{g}_\ell = \alpha^{\ell-1}\hat{g}_1, \quad 2 \le \ell \le T. \tag{22}$$

In other words, once the first channel estimate $\hat{g}_1$ is obtained during pilot transmission, the remaining channel estimates in the data block linearly weigh $\hat{g}_1$ by an appropriate power of α, depending on how far they are from the pilot symbol. It is clear that for faster channels (α being closer to zero) the quality of channel estimate deteriorates rapidly as we proceed through the data block.

V. Data Transmission Mode and Channel Capacity

In the data transmission mode, the SNR is degraded by the channel estimation errors. To see this, let us rewrite (1) after channel estimation as

$$y_\ell = g_\ell x_\ell + n_\ell \tag{23}$$

$$= \underbrace{\hat{g}_\ell x_\ell}_{\text{signal}} + \underbrace{\tilde{g}_\ell x_\ell + n_\ell}_{\text{noise}}. \tag{24}$$

In particular, the data power is reduced from $\sigma_g^2\mathcal{E}_d$ to $\sigma^2_{\hat{g}}(\ell)\mathcal{E}_d$, because $\sigma^2_{\hat{g}}(\ell) \le \sigma_g^2$. Moreover, the noise power is increased from N_0 to $N_0 + M(\ell)\mathcal{E}_d$. Therefore, we can define the effective instantaneous SNR in the data transmission mode at each time index ℓ as

$$\rho_{\text{inst}}(\ell) = \frac{|\hat{g}_\ell|^2\mathcal{E}_d}{\sigma^2_{\hat{g}}(\ell)\mathcal{E}_d + N_0}. \tag{25}$$

We note that $\lambda_\ell \triangleq |\hat{g}_\ell|^2$ is the instantaneous square magnitude of channel estimate at time index ℓ. Uisng the realtionship between $\hat{g}_\ell$ and $\hat{g}_1$ in (22), we can write $\lambda_\ell \triangleq \alpha^{2(\ell-1)}\lambda_1$, where $\lambda_1 \triangleq |\hat{g}_1|^2$ is the instantaneous square magnitude of channel estimate at pilot transmission. Now, by multiplying the numerator and denominator by σ_g^2/N_0 and using the definition of ρ_d in (11) and (20)-(21), we can rewrite (25) as

$$\rho_{\text{inst}}(\ell) = \frac{\alpha^{2(\ell-1)}\lambda_1\frac{1-\gamma}{1-\eta}\rho}{M(\ell)\frac{1-\gamma}{1-\eta}\rho + \sigma_g^2}. \tag{26}$$

A closed-form expression for the information capacity of the time-varying Gauss-Markov fading channel in the presence of

imperfect channel estimation is still unavailable. As discussed in the Introduction, a common approach in the literature is to study a lower bound to the channel capacity. In this case, the instantaneous capacity lower bound at time index ℓ given the first channel estimate $\lambda_1 = |\hat{g}_1|^2$ is

$$\begin{aligned} C_{\mathrm{LB}}(\ell, \lambda_1) &= \log\big(1 + \rho_{\mathrm{inst}}(\ell)\big) \\ &= \log\Big(1 + \frac{\alpha^{2(\ell-1)}\lambda_1 \frac{1-\gamma}{1-\eta}\rho}{M(\ell)\frac{1-\gamma}{1-\eta}\rho + \sigma_g^2}\Big), \end{aligned} \tag{27}$$

where we assume worst-case Gaussian noise [6] and Gaussian input distribution to obtain the lower bound.

We note the capacity lower bound in (27) is a function of time index ℓ. Therefore, the lower bound is different from those studied in [4], [5], [7], where the channel estimation MMSE and hence, the capacity lower bound were independent of the time index and calculated for a band-limited FFC process. In our case, the capacity lower bound per transmission block given the first channel estimate $\lambda_1 = |\hat{g}_1|^2$ is

$$C_{\mathrm{LB}}(\lambda_1) = \frac{1}{T}\sum_{\ell=2}^{T} C_{\mathrm{LB}}(\ell, \lambda_1). \tag{28}$$

Now, the ergodic capacity lower bound is the expected value of $C_{\mathrm{LB}}(\lambda_1)$ over all possible exponentially distributed λ_1 and is given as

$$\overline{C}_{\mathrm{LB}} = \int_0^\infty C_{\mathrm{LB}}(\lambda_1) f(\lambda_1) d\lambda_1, \tag{29}$$

where $f(\lambda_1)$ is defined to be

$$f(\lambda_1) = \frac{1}{\sigma_g^2 - M(1)} \exp\Big(-\frac{\lambda_1}{\sigma_g^2 - M(1)}\Big). \tag{30}$$

VI. Numerical Results

The expressions for the channel estimation MMSE in (20) and hence, the capacity lower bound are involved. As a result, we do not aim to optimize the pilot power ratio or pilot spacing analytically. Instead, we numerically optimize PSAM parameters for a wide and practical range of FFC rates and SNR budget. We will denote the optimum pilot power allocation ratio and pilot spacing (that maximize the capacity lower bound in (29)) by γ^* and η^*, respectively.

Fig. 1 shows the 3D plot of the capacity lower bound for the SNR budget of $\rho = \sigma_g^2\mathcal{E}/N_0 = 10$ dB and at the normalized fading rate of $f_D T_s = 0.1$. The Gauss-Markov parameter α is evaluated using $\alpha = J_0\big(2\pi f_D T_s\big) = 0.9037$. The optimum capacity lower bound is obtained at $\eta^* = 0.25$ (or $T = 4$) and $\gamma^* = 0.37$. That is, for every $T^* - 1 = 3$ data symbols, one pilot symbol should be transmitted. This is due to the fact that the FFC is relatively fast and frequent pilot transmission is required to maintain reliable data decoding. From this figure, we also observe that the lower bound is more sensitive to the pilot spacing η than to the pilot power allocation ratio and decreases considerably for large block lengths T, whereas, it is more or less constant for a wide range of pilot power allocation between about $\gamma = 0.15$ and $\gamma = 0.65$ with less than 10% decrease in the capacity lower bound in this range.

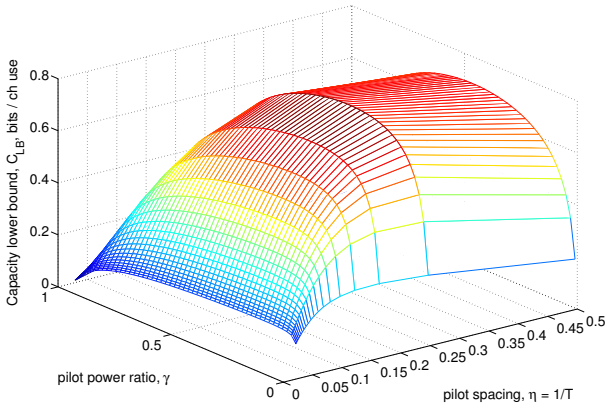

Fig. 1. The 3D plot of the capacity lower bound defined in (29) for the average SNR budget of $\rho = \sigma_g^2\mathcal{E}/N_0 = 10$ dB and at the normalized fading rate of $f_D T_s = 0.1$. The Gauss-Markov parameter α is evaluated using $\alpha = J_0\big(2\pi f_D T_s\big) = 0.9037$. The lower bound is more sensitive to the pilot spacing η than to the pilot power allocation ratio and decreases considerably for large block lengths T, whereas, it is more or less constant for a wide range of pilot power allocation between about $\gamma = 0.15$ and $\gamma = 0.65$ with less than 10% decrease in the capacity lower bound in this range.

With the optimum values for the pilot spacing and pilot power ratio, the average SNR per pilot symbol is given using (10) as $\rho_p = 11.70$ dB and the average SNR per data symbol is given using (11) to be $\rho_d = 9.24$ dB.

Fig. 2 shows the optimum normalized allocation of power to pilot symbol $\mathcal{E}_p/\mathcal{E} = \gamma^*/\eta^*$ for a wide range of SNR budget $\rho = \sigma_g^2\mathcal{E}/N_0$ and normalized fading rates $f_D T_s$. Two main observations are made from the curves in this figure. First, it is clear that the optimum normalized allocation of power to the pilot symbol is more sensitive to the operating SNR in the slowest fading channel at $f_D T_s = 0.01$. Whereas, the optimum normalized allocation of power to pilot symbol is almost constant for the SNR range for the fastest fading rate studied at $f_D T_s = 0.15$. Second, apart from some local fluctuations, the optimum normalized allocation of power to the pilot symbol decreases as SNR increases. That is, relatively speaking, a lesser fraction of the power is required to be spent for the pilot transmission in high SNR. This is in accordance with our expectation that channel estimation at high SNR is less challenging and requires less available resources.

Fig. 3 shows the optimum block length $T^* = 1/\eta^*$ for a wide range of SNR budget $\rho = \sigma_g^2\mathcal{E}/N_0$ and normalized fading rates $f_D T_s$. Similar to Fig. 2, the optimum block length is very sensitive to SNR in the slowest fading channel at $f_D T_s = 0.01$. Whereas, the optimum block length is constant for the two faster fading rates of $f_D T_s = 0.11$ and $f_D T_s = 0.15$. We also observe that the optimum block length decreases or stays constant as SNR increases. Finally, looking vertically at the curves, we note that the optimum block length dramatically decreases as the fading rate increases. As expected, for faster fading conditions, more frequent pilot symbols are required.

Fig. 4 presents the lower bound on channel capacity (defined

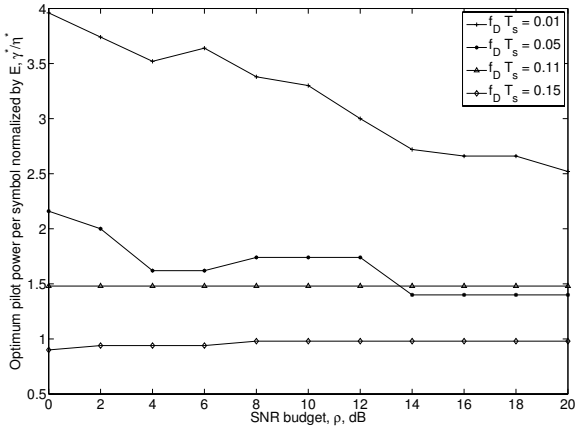

Fig. 2. The optimum normalized allocation of power to the pilot symbol $\mathcal{E}_p/\mathcal{E} = \gamma^*/\eta^*$ for a wide range of SNR budget ρ and normalized fading rates. First, it is clear that the optimum normalized allocation of power to pilot symbol is more sensitive to the SNR in the slowest fading channel at $f_D T_s = 0.01$. Apart from some local fluctuations, less normalized fraction of power is required to be spent for pilot transmission at high SNR.

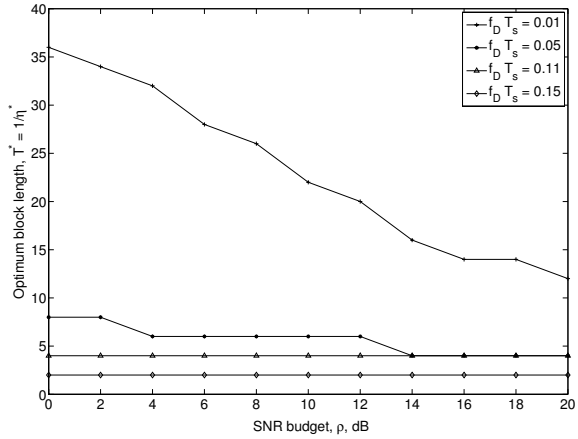

Fig. 3. The optimum block length $T^* = 1/\eta^*$ as a function of the SNR budget and the normalized fading rate. The optimum block length is very sensitive to the SNR in the slowest fading channel at $f_D T_s = 0.01$. In all fading rate conditions, the optimum block length decreases or stays constant as SNR increases. Looking vertically at the curves, more frequent pilot symbols are required for faster fading conditions.

in (29)) as a function of the SNR budget $\rho = \sigma_g^2 \mathcal{E}/N_0$ and the normalized fading rate $f_D T_s$. For comparison, we have also shown the capacity lower bound with equal power allocation strategy discussed in Section III-D, which is only optimized for the pilot spacing η^*. We note that for the faster fading rates of $f_D T_s = 0.05$ and $f_D T_s = 0.11$, using the simple equal power allocation does not incur a noticeable capacity loss, *provided that we optimize over the pilot spacing* η. However, for the slowest fading channel at $f_D T_s = 0.01$, equal power strategy incurs a noticeable capacity loss, even when we optimize over the pilot spacing η. However, the SNR gap between capacity

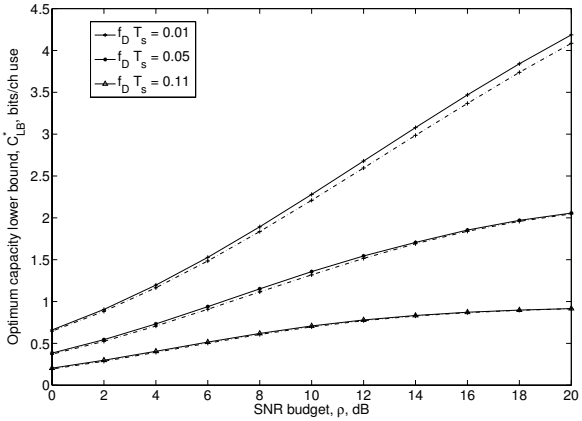

Fig. 4. The lower bound on channel capacity $\overline{C}_{\mathrm{LB}}$ defined in (29) as a function of the SNR budget and the normalized fading rate. The solid curves show the optimal power allocation scheme and the dashed curves show the suboptimal equal power allocation scheme. We note that for the faster fading rates of $f_D T_s = 0.05$ and $f_D T_s = 0.11$, using the simple equal power allocation does not incur a noticeable capacity loss, *provided that we optimize over the pilot spacing* η. However, for the slowest fading channel at $f_D T_s = 0.01$, equal power strategy incurs a noticeable capacity loss, even when we optimize over the pilot spacing η. The SNR gap between capacity curves is at most 1 dB for the very high SNR range.

curves is at most 1 dB for the very high SNR range. We also studied the second alternative power allocation scheme, namely power ramping described in Section III-D. However, we observed that this method does not provide any noticeable advantage in terms of the capacity lower bound. Therefore, for more clarity of the curves, we have omitted the corresponding curves in Fig. 4.

Finally, we investigate the sensitivity of the capacity lower bound to the choice of power allocation ratio γ and pilot spacing η. Fig. 5 shows the capacity lower bound versus power allocation ratio γ for two slow and fast fading channels at two low and high SNR conditions. Fig. 5 confirms our earlier finding that PSAM transmission scheme is more sensitive to the choice of γ for the slower fading case. Fig. 6 shows the capacity lower bound sensitivity to pilot spacing η for the low SNR case of $\rho = 0$ dB. We note that the lower bound stays almost constant for $\eta > 0.15$ at the normalized fading rate $f_D T_s = 0.1$. However, any less frequent pilot spacing dramatically reduces the lower bound towards zero and should be avoided.

VII. Conclusions

In this paper, we studied the optimal design of PSAM from an information-theoretic viewpoint in time-varying Gauss-Markov flat-fading channels. To this end, we examined a lower bound on the channel information capacity, which was based on the steady-state MMSE in PSAM channel estimation and prediction using the Kalman filtering. The parameters that were available for the maximization of the capacity lower bound were the power ratio and the fraction of time allocated to pilot symbol transmission. Our analysis showed that this

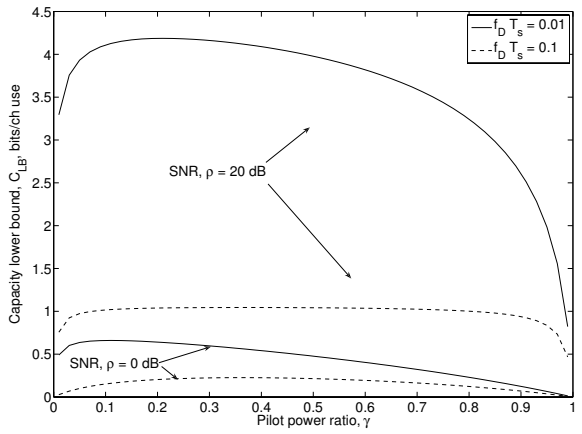

Fig. 5. The capacity lower bound versus power allocation ratio γ for two slow and fast fading channels at two low and high SNR conditions. This figure confirms our earlier finding that PSAM transmission scheme is more sensitive to the choice of γ for the slower fading channel.

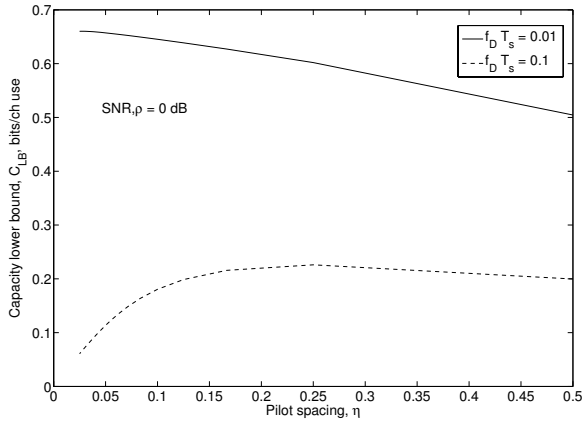

Fig. 6. The capacity lower bound versus pilot spacing η for two slow and fast fading channels at two low and high SNR conditions. We note that the lower bound stays almost constant for $\eta > 0.15$ at the normalized fading rate $f_D T_s$, any less frequent pilot spacing dramatically reduces the lower bound towards zero and should be avoided.

capacity lower bound is more sensitive to the pilot power allocation ratio in relatively slow Gauss-Markov fading channels (with the normalized fading rate $f_D T_s \simeq 0.01$). We observed that for such slow fading rates, optimal power allocation and optimal pilot spacing are more sensitive to the operating SNR. Whereas, for faster fading channels, optimal parameters stay more or less constant for the SNR range considered. We also compared the optimal pilot power allocation scheme with alternative power allocation strategies, such as equal power strategy. We observed that the equal power allocation strategy is suboptimal by at most 1 dB for the slow fading rate of $f_D T_s = 0.01$. In faster fading channels, however, equal power allocation does not incur a noticeable loss in the capacity lower bound.

ACKNOWLEDGMENTS

This work was supported under Australian Research Council's Discovery Projects funding scheme (project number DP0773898). The authors wish to thank Tharaka Lamahewa for helpful discussions.

REFERENCES

[1] J. K. Cavers, "An analysis of pilot symbol assisted modulation for Rayleigh fading channels," *IEEE Trans. Veh. Technol.*, vol. 40, no. 4, pp. 686–693, Nov. 1991.

[2] S. M. Redl, M. K. Weber, and M. W. Oliphan, *An Introduction to GSM*, 1st ed. Boston: Artech House, 1995.

[3] M. Medard, "The effect upon channel capacity in wireless communications of perfect and imperfect knowledge of the channel," *IEEE Trans. Inform. Theory*, vol. 46, no. 3, pp. 933–946, May 2000.

[4] S. Ohno and G. B. Giannakis, "Average-rate optimal PSAM transmissions over time-selective fading channels," *IEEE Trans. Wireless Commun.*, vol. 1, no. 4, pp. 712–720, Oct. 2002.

[5] X. Deng and A. M. Haimovich, "On pilot symbol aided channel estimation for time varying rayleigh fading channels," in *Proc. 38th Annual Conf. on Inform. Sciences and Systems (CISS)*, Princeton, NJ, Mar. 2004.

[6] B. Hassibi and B. M. Hochwald, "How much training is needed in multiple-antenna wireless links?" *IEEE Trans. Inform. Theory*, vol. 49, no. 4, pp. 951–963, Apr. 2003.

[7] J. Baltersee, G. Fock, and H. Meyr, "An information theoretic foundation of synchronized detection," *IEEE Trans. Commun.*, vol. 49, no. 12, pp. 2115–2123, Dec. 2001.

[8] M. Dong, L. Tong, and B. M. Sadler, "Optimal insertion of pilot symbols for transmissions over time-varying flat fading channels," *IEEE Trans. Signal Processing*, vol. 52, no. 5, pp. 1403–1418, May 2004.

[9] R. H. Clarke, "A statistical theory of mobile-radio reception," *Bell Syst. Tech. J.*, vol. 47, no. 6, pp. 957–1000, 1968.

[10] R. Chen, B. Hajek, R. Koetter, and U. Madhow, "On fixed input distributions for noncoherent communication over high-SNR Rayleigh-fading channels," *IEEE Trans. Inform. Theory*, vol. 50, no. 12, pp. 3390–3396, Dec. 2004.

[11] K. E. Baddour and N. C. Beaulieu, "Autoregressive models for fading channel simulation," in *Proc. IEEE Global Commun. Conf. (GLOBECOM)*, San Antonio, TX, Nov. 2001, pp. 1187–1192.

[12] J. G. Proakis, *Digital Communications*, 4th ed. New York: Mc Graw Hill, 2000.